Coupling tabulated chemistry with compressible CFD solvers

Ronan Vicquelin, Benoit Fiorina, Sandra Payet, Nasser Darabiha, Olivier Gicquel

Coupling tabulated chemistry with compressible CFD solvers

R. Vicquelin[a,b,*], B. Fiorina[a], S. Payet[b], N. Darabiha[a], O. Gicquel[a]

[a] *Laboratoire EM2C-CNRS, Ecole Centrale Paris 92295 Châtenay Malabry, France*
[b] *GDF SUEZ, Pôle CHENE, Centre de Recherche et d'Innovation Gaz et Energies Nouvelles, 93211 Saint-Denis la Plaine, France*

Abstract

The present work focuses on the coupling between tabulated chemistry techniques with compressible solvers. In low Mach-number CFD solvers the coupling is straightforward because thermo-chemical quantities are directly read in a thermo-chemical database. However, because of perturbations introduced by acoustics, the coupling with fully compressible Navier-Stokes equations is not straightforward. In order to be consistent with tabulated chemistry framework, a new strategy to predict temperature field from the transported energy is developed. Boundary conditions are reformulated following Navier-Stokes Characteristic Boundary Conditions (NSCBC) formalism. The method called TTC (Tabulated Thermo-chemistry for Compressible flows) is implemented in a compressible CFD code and validated by comparison with multi-component simulations. Temperature computation and characteristic boundary conditions reformulations are first validated on one-dimensional tests. A three-dimensional non-reactive case is then computed by performing a large eddy simulation of a turbulent round jet. Finally, a one-dimensional laminar flame simulation assesses the method performances.

Keywords: tabulated chemistry, compressible flow, characteristic boundary conditions

1. Introduction

Large Eddy Simulation (LES) has become an affordable tool. This major evolution is due to the important improvement of the available computational power during the last decade. Using parallel computational resources, Boileau *et al*. [1] were able to simulate the ignition of a full combustion chamber. Similar simulations of realistic systems were also performed by [2, 3]. All these works are of great interest to study turbulent flame dynamics, combustion instabilities or mixing characterization but they are limited in terms of chemistry description.

Indeed, because of large number of species, detailed chemistry simulations remain too expensive in terms of CPU time to be achieved in such configurations. Some direct numerical simulations have been done using detailed chemistry mechanisms for hydrogen-air flames [4] or methane-air flames [5] but they are limited to very small configurations that are far from industrial needs.

A classical approach used to take into account detailed chemistry effects in realistic LES for a low CPU cost is to use tabulated chemistry. Tabulated chemistry methods assume that chemical evolutions in the composition space can be parameterized and tabulated by a reduced set of variables $(\psi_1, ..., \psi_n)$ where n is the number of chemical database coordinates. In general, ψ_l are combinations of species mass fractions. Knowing these variables in a simulation, all thermo-chemical variables φ can then be estimated by using the chemical database $\varphi^{tab}(\psi_1, ..., \psi_n)$. Among these tabulation techniques one can mention ILDM [6], FPI [7], FGM [8], REDIM [9] or ICE-PIC [10] methods. In these methods, instead of solving one balance equation for each chemical species involved in the detailed elementary reactions, only few equations for the reduced set of variables are solved.

The main problem when coupling this procedure with compressible Navier-Stokes equations is that perturbations due to compressibility effects are not considered during the database generation. This limitation is not a problem if the CFD solver is based on a low Mach-number assumption where the introduction of tabulated chemistry is straightforward [11, 12, 13]. But introducing tabulated chemistry in a compressible CFD solver is more challenging. In this case, temperature can not

*Corresponding author
Email addresses: ronan.vicquelin@centraliens.net (R. Vicquelin), benoit.fiorina@em2c.ecp.fr (B. Fiorina), sandra.payet@gdfsuez.com (S. Payet), nasser.darabiha@em2c.ecp.fr (N. Darabiha), olivier.gicquel@em2c.ecp.fr (O. Gicquel)

be directly read in the database because the tabulated temperature does not take into account acoustic perturbations. Galpin *et al*. [14] have proposed to solve, in addition to the reduced set of variables, balance equations for some chemical species selected to estimate the temperature from energy. For methane-air combustion, the number of supplemental species required to have a fair estimate of the temperature is nine [14]. Therefore this technique leads to a large increase of the number of equations. In addition, a divergence between the additional transported species and the tabulated ones is frequently observed and requires specific treatment. A second problem in compressible codes is the interaction between acoustics and boundaries [15, 16]. When using tabulated chemistry, boundary conditions for the reduced set of variables should therefore take into account perturbations due to acoustics.

In the present work, a new technique called TTC (Tabulated Thermochemistry for Compressible flows) is developed to introduce tabulated chemistry strategies in compressible solvers. This approach only requires to solve additional balance equations for the database coordinates. First, the governing equations of reactive flow described by tabulated chemistry are briefly presented and a method is proposed to take into account temperature deviation due to acoustics. Then characteristic boundary condition treatment is detailed for tabulated chemistry. Finally, validation tests are presented. Reformulation of temperature computation and boundary treatment are validated with 1-D tests by comparison with multi-component simulations. Further validations are conducted by performing a non-reactive 3-D large eddy simulation of a round jet and a reactive case where the FPI tabulation method is chosen to reproduce a 1-D laminar flame.

2. Governing equations for tabulated chemistry

Conservative variables are gathered in the vector $\boldsymbol{U} = (\rho, \rho u_i, \rho e_t, \rho\psi_1, ..., \rho\psi_n)^\top$ where ρ is the mass density, u_i are the velocity components, $e_t = u_i u_i/2 + e$ is the total energy, sum of kinetic and internal energy, and ψ_l is the l^{th} coordinate used to describe the thermochemical database. In multi-component formulation, mixture internal energy e is given as $e = \sum_{k=1}^{N} e_k Y_k$ where N is the number of species and Y_k, e_k are the k^{th} species mass fraction and energy, respectively. At a given temperature T, e_k reads:

$$e_k = \int_{T_0}^{T} C_{vk}(T)\mathrm{d}T - \frac{RT_0}{W_k} + \Delta h^0_{f,k} \tag{1}$$

where $R = 8.314$ J/mol/K is the ideal gas constant, C_{vk} is the species specific heat capacity at constant volume, W_k is the k^{th} species molar mass, $\Delta h^0_{f,k}$ is the species enthalpy of formation and T_0 is the reference temperature ($T_0 = 298$ K).

When using tabulated chemistry, governing equations for adiabatic reactive flows can be written as:

$$\frac{\partial \boldsymbol{U}}{\partial t} + \frac{\partial \boldsymbol{F}^j}{\partial x_j} + \frac{\partial \boldsymbol{F}^j_d}{\partial x_j} = \boldsymbol{S} \tag{2}$$

where the source term vector is $\boldsymbol{S} = (0, 0, 0, 0, 0, \dot{\omega}_{\psi_1}, ..., \dot{\omega}_{\psi_n})^\top$ with $\dot{\omega}_{\psi_l}$ the chemical mass production rate of the variable ψ_l. $\boldsymbol{F}^j$ and $\boldsymbol{F}^j_d$ are respectively the Eulerian and diffusion fluxes in direction j:

$$\boldsymbol{F}^j = \begin{pmatrix} \rho u_j \\ \rho u_j u_1 + \delta_{1j} P \\ \rho u_j u_2 + \delta_{2j} P \\ \rho u_j u_3 + \delta_{3j} P \\ u_j(\rho e_t + P) \\ \rho u_j \psi_1 \\ \vdots \\ \rho u_j \psi_n \end{pmatrix} \quad , \quad \boldsymbol{F}^j_d = \begin{pmatrix} 0 \\ -\tau_{1j} \\ -\tau_{2j} \\ -\tau_{3j} \\ -u_i\tau_{ij} + q_j \\ -\rho D_1 \frac{\partial \psi_1}{\partial x_j} \\ \vdots \\ -\rho D_n \frac{\partial \psi_n}{\partial x_j} \end{pmatrix} \tag{3}$$

where δ_{ij} is the Kronecker operator: $\delta_{ij} = 1$ for $i = j$ and $\delta_{ij} = 0$ for $i \neq j$. P is the thermodynamic pressure given by the ideal gas law, $P = \rho RT/W$, where $W = \left(\sum_{k=1}^{N} Y_k/W_k\right)^{-1}$ is the mixture molar mass. τ_{ij} is the viscous tensor, q_j is the heat flux and ψ_l follows a Fick diffusion law with diffusivity coefficient D_l. The fluid is considered as Newtonian. The heat flux vector is given using Fourier law and assuming unity Lewis number for species diffusion:

$$q_j = -\frac{\lambda}{C_p}\frac{\partial h}{\partial x_j} \tag{4}$$

where $h = e + P/\rho$ is the mixture enthalpy, λ is the mixture thermal conductivity. C_p and C_v are the mixture specific heat capacities at constant pressure and constant volume respectively. The ratio of heat capacities $\gamma = C_p/C_v$ is introduced. Diffusivity coefficients D_l are computed by assuming unity Lewis number: $D_l = D = \frac{\lambda}{\rho C_p}$. The coupling strategy developed in this article is not affected by this assumption.

In tabulated chemistry framework, C_p, C_v, λ and D are stored in a look-up table as a function of $(\psi_1, ..., \psi_n)$. A technique adapted to tabulated chemistry to estimate the temperature from the transported energy is proposed in the following section.

3. Temperature computation with tabulated chemistry

Conservative variables ρ, ρu_i, ρe_t and $\rho\psi_l$ are solved from their respective balance equations. The remaining difficulty is the computation of temperature. In low Mach-number approach, as pressure fluctuations are assumed to be small, the temperature is directly extracted from the database: $T = T^{tab}(\psi_1, ..., \psi_n)$. This assumption is not accurate when compressibility effects are taken into account. Indeed, in this case, the transported values of e and T are different from the tabulated ones: e^{tab} and T^{tab}. A solution to compute the temperature is to approximate the fluid composition by a reduced sample of species as proposed by Galpin *et al.* [14]. It prevents a prohibitive storage in the database of all species thermodynamical properties and mass fractions. However, as mentioned previously, this method presents several drawbacks. Another solution is to tabulate the energy as a function of database coordinates and temperature. An additional coordinate (the temperature) needs therefore to be added to the chemical table and an iterative algorithm is required to deduce the temperature from energy. Such an approach is memory space and CPU time consuming. A less expensive alternative is here proposed.

The first order truncated Taylor expansion of e around $T = T^{tab}$ leads to the following linear approximation to estimate the temperature in TTC formalism:

$$T = T^{tab}(\psi_1, ..., \psi_n) + \frac{e - e^{tab}(\psi_1, ..., \psi_n)}{C_v^{tab}(\psi_1, ..., \psi_n)} \qquad (5)$$

The "compressible" temperature T can therefore be approximated from the tabulated energy and temperature e^{tab} and T^{tab}, respectively and the transported energy $e = e_t - u_i u_i/2$. Note that this assumption is valid in the case of moderate acoustic perturbations which induce small temperature variations. It is justified when combustion operates at constant pressure such as in gas turbines, furnaces, unconfined laboratory flames, etc... Other realistic situations exist where pressure variations are sufficiently large to affect the chemistry (internal combustion engines, detonation waves, ...) and extra-coordinates have to be added to the chemical database.

4. Characteristic boundary conditions for tabulated chemistry

4.1. Characteristic wave treatment

In compressible CFD solvers, boundary conditions are provided using characteristic boundary conditions. Navier-Stokes Characteristic Boundary Conditons (NSCBC) have been first derived for single-component flows [15], and later for multi-component flows [16]. As N species transport equations have been replaced by $n < N$ equations for variables ψ_l, characteristic wave decomposition must be expressed in terms of n characteristic waves corresponding to ψ_l and not N species waves anymore in TTC formalism. For that purpose, Eq. (2) is written introducing the vector of non-conservative variables $\boldsymbol{V} = (\rho, u_i, P, \psi_1, ..., \psi_n)^\top$:

$$\frac{\partial \boldsymbol{V}}{\partial t} + \boldsymbol{A}^j \frac{\partial \boldsymbol{V}}{\partial x_j} + \boldsymbol{J}^{-1} \frac{\partial \boldsymbol{F}_d^j}{\partial x_j} = \boldsymbol{J}^{-1} \boldsymbol{S} \qquad (6)$$

where $\boldsymbol{A}^j$ is a $(n+5) \times (n+5)$ matrix:

$$\boldsymbol{A}^j = \begin{pmatrix} u_j & \rho\delta_{1j} & \rho\delta_{2j} & \rho\delta_{3j} & 0 & 0 & \cdots & 0 \\ 0 & u_j & 0 & 0 & \frac{1}{\rho}\delta_{1j} & 0 & \cdots & 0 \\ 0 & 0 & u_j & 0 & \frac{1}{\rho}\delta_{2j} & 0 & \cdots & 0 \\ 0 & 0 & 0 & u_j & \frac{1}{\rho}\delta_{3j} & 0 & \cdots & 0 \\ 0 & \rho a^2\delta_{1j} & \rho a^2\delta_{2j} & \rho a^2\delta_{3j} & u_j & 0 & \cdots & 0 \\ 0 & 0 & 0 & 0 & 0 & u_j & \cdots & 0 \\ \vdots & \vdots & \vdots & \vdots & \vdots & \vdots & \ddots & \vdots \\ 0 & 0 & 0 & 0 & 0 & 0 & \cdots & u_j \end{pmatrix}$$

. $a = (\gamma r T)^{1/2}$ is the speed of sound and $r = R/W$. The jacobian matrix $\boldsymbol{J} = \frac{\partial \boldsymbol{U}}{\partial \boldsymbol{V}}$ reads:

$$\boldsymbol{J} = \begin{pmatrix} 1 & 0 & 0 & 0 & 0 & 0 & \cdots & 0 \\ u_1 & \rho & 0 & 0 & 0 & 0 & \cdots & 0 \\ u_2 & 0 & \rho & 0 & 0 & 0 & \cdots & 0 \\ u_3 & 0 & 0 & \rho & 0 & 0 & \cdots & 0 \\ e_t - \frac{rT}{\beta} & \rho u_1 & \rho u_2 & \rho u_3 & \frac{1}{\beta} & -\frac{\rho}{\beta}\vartheta_{\psi_1} & \cdots & -\frac{\rho}{\beta}\vartheta_{\psi_n} \\ \psi_1 & 0 & 0 & 0 & 0 & \rho & \cdots & 0 \\ \vdots & \vdots & \vdots & \vdots & \vdots & \vdots & \ddots & \vdots \\ \psi_n & 0 & 0 & 0 & 0 & 0 & \cdots & \rho \end{pmatrix}$$

where $\beta = \gamma - 1$ and ϑ_{ψ_l} is defined as:

$$\vartheta_{\psi_l} = \sum_{k=1}^{N} \left(\frac{RT}{W_k} - \beta e_k \right) \frac{\partial Y_k}{\partial \psi_l} \qquad (7)$$

Assuming that the boundary normal direction is along the x_1 axis, Eq. (6) is written as:

$$\frac{\partial \boldsymbol{V}}{\partial t} + \boldsymbol{A}^1 \frac{\partial \boldsymbol{V}}{\partial x_1} = \text{RHS} \qquad (8)$$

where RHS= $\boldsymbol{J}^{-1}\boldsymbol{S} - \boldsymbol{J}^{-1}\frac{\partial \boldsymbol{F}_d^j}{\partial x_j} - \boldsymbol{A}^2\frac{\partial \boldsymbol{V}}{\partial x_2} - \boldsymbol{A}^3\frac{\partial \boldsymbol{V}}{\partial x_3}$. Matrix $\boldsymbol{A}^1$ has $5 + n$ eigenvalues λ^m which are given here with

one example of right eigenvectors r_m:

$$\begin{aligned}
\lambda^1 = u_1 + a, \quad & r_1 = \quad (\frac{\rho}{2a}, \frac{1}{2}, 0, 0, \frac{\rho a}{2}, 0, ..., 0)^\top \\
\lambda^2 = u_1, \quad & r_2 = \quad (1, 0, 0, 0, 0, 0, ..., 0)^\top \\
\lambda^3 = u_1, \quad & r_3 = \quad (0, 0, 1, 0, 0, 0, ..., 0)^\top \\
\lambda^4 = u_1, \quad & r_4 = \quad (0, 0, 0, 1, 0, 0, ..., 0)^\top \\
\lambda^5 = u_1 - a, \quad & r_5 = \quad (\frac{\rho}{2a}, -\frac{1}{2}, 0, 0, \frac{\rho a}{2}, 0, ..., 0)^\top \\
\lambda^6 = u_1, \quad & r_6 = \quad (0, 0, 0, 0, 0, 1, ..., 0)^\top \\
& \quad ... \\
\lambda^{5+n} = u_1, \quad & r_{5+n} = \quad (0, 0, 0, 0, 0, 0, ..., 1)^\top
\end{aligned}$$

The right eigenvectors r_m are gathered in the transformation matrix $\boldsymbol{R}$ in columns. Inverting $\boldsymbol{R}$ gives the matrix $\boldsymbol{L}$ whose lines are the left eigenvectors l_m. Amplitude time variations of characteristic waves are defined as $\mathscr{L}_m = \lambda^m l_m \frac{\partial V}{\partial x_1}$ [17] and are gathered in the vector $\mathscr{L}$:

$$\mathscr{L} = \begin{pmatrix} \lambda^1 \left(\frac{\partial u_1}{\partial x_1} + \frac{1}{\rho a} \frac{\partial P}{\partial x_1} \right) \\ \lambda^2 \left(\frac{\partial \rho}{\partial x_1} - \frac{1}{a^2} \frac{\partial P}{\partial x_1} \right) \\ \lambda^3 \frac{\partial u_2}{\partial x_1} \\ \lambda^4 \frac{\partial u_3}{\partial x_1} \\ \lambda^5 \left(-\frac{\partial u_1}{\partial x_1} + \frac{1}{\rho a} \frac{\partial P}{\partial x_1} \right) \\ \lambda^6 \frac{\partial \psi_1}{\partial x_1} \\ ... \\ \lambda^{5+n} \frac{\partial \psi_n}{\partial x_1} \end{pmatrix} \tag{9}$$

Eq. (8) can then be reformulated as:

$$\frac{\partial \boldsymbol{V}}{\partial t} + \boldsymbol{R}\mathscr{L} = \text{RHS} \tag{10}$$

Eq. (10) specifies boundary conditions on the characteristic waves amplitudes $\mathscr{L}_m$. Indeed, if transverse, diffusion and source terms are neglected, i.e. RHS = 0, the Local One Dimensional Inviscid system [15] is retrieved. Once $\mathscr{L}_m$ are known, conservation equations are expressed to provide Navier-Stokes Characteristic Boundary Conditions (NSCBC) at the boundary face:

$$\frac{\partial \boldsymbol{U}}{\partial t} + \boldsymbol{J}\boldsymbol{R}\mathscr{L} + \frac{\partial \boldsymbol{F}^2}{\partial x_2} + \frac{\partial \boldsymbol{F}^3}{\partial x_3} + \frac{\partial \boldsymbol{F}_d^j}{\partial x_j} = \boldsymbol{S} \tag{11}$$

4.2. Tabulation of ϑ_{ψ_l}

The terms defined by Eq. (7) need to be computed at the boundary but can not be directly tabulated since they depend on temperature and energy which are both sensitive to compressible effects. Consequently, as done for temperature correction in Eq. (5), ϑ_{ψ_l} is compared to its corresponding tabulated value. The difference $\Delta\vartheta_{\psi_i} = \vartheta_{\psi_i} - \vartheta^{tab}_{\psi_i}(\psi_1, ..., \psi_n)$ is approximated following a linear approximation by:

$$\Delta\vartheta_{\psi_l} \approx \sum_{k=1}^{N} \left(\frac{R}{W_k} - \beta C_{vk} \right) \frac{\partial Y_k}{\partial \psi_l} \left[T - T^{tab}(\psi_1, ..., \psi_n) \right] \tag{12}$$

Therefore, $\vartheta^{tab}_{\psi_l}$ and $\sigma^{tab}_{\psi_l} = \sum_{k=1}^{N} (R/W_k - \beta C_{vk}) \frac{\partial Y_k}{\partial \psi_l}$ are first stored in a look-up table as a function of $(\psi_1, ..., \psi_n)$. Then to introduce compressible effects in the simulation, ϑ_{ψ_l} is computed as:

$$\vartheta_{\psi_l} = \vartheta^{tab}_{\psi_l}(\psi_1, ..., \psi_n) + \sigma^{tab}_{\psi_l}(\psi_1, ..., \psi_n)(T - T^{tab}) \tag{13}$$

5. Validation tests

The present method to introduce tabulated chemistry into a compressible CFD solver is validated. For that purpose, the temperature and characteristic boundary condition corrections presented in sections 3 and 4 are tested. First, the temperature correction method is validated by performing a one-dimensional simulation in the case of an acoustic wave traveling a gas mixture at rest. Then, the NSCBC terms corrections are validated by sending acoustic and entropic waves through boundaries. Finally, a turbulent jet and a laminar premixed flame are simulated to illustrate the model performances. For all these validations two simulations are performed. The first one uses multi-component transport formulation for the four species present in the mixture (reference simulation), while the other one uses tabulated chemistry following the TTC formalism. All simulations are done with the compressible CFD solver AVBP [19] using a third-order numerical scheme [20].

In the database used for non-reactive test cases, all thermo-chemical quantities are stored in a look-up table in term of a unique coordinate: $n = 1$ and $\psi_1 = z$ where z is the mixture fraction. This database represents a rich methane-air mixture ($z = 1$ with equivalence ratio $\phi = 4.4$) injected in a hot vitiated air ($z = 0$) coflow produced by the lean combustion of a hydrogen-air mixture ($\phi = 0.4$). Table 1 details species mass fractions and temperature on the fuel side (Y_{k_f} and T_f) and on the oxidizer side ($Y_{k_{ox}}$ and T_{ox}). Species mass fractions and temperature are stored in the database as:

$$Y_k(z) = (Y_{k_f} - Y_{k_{ox}})z + Y_{k_{ox}} \tag{14}$$

and

$$T(z) = (T_f - T_{ox})z + T_{ox} \tag{15}$$

In the present case only one balance equation for the mixture fraction z is added to the mass, momentum and energy balance equations.

5.1. Temperature correction test

The compressible deviation correction of temperature introduced by Eq. (5) is validated by computing an acoustic wave traveling across a periodic domain of length $L = 0.005$ m in a pure oxidizer mixture ($z_0 = 0$, Y_{k_0}, T_0, $P_0 = 1$ atm). The initial solution is given by:

$$\begin{aligned} u &= \pm A \exp\left(-\frac{(x-x_0)^2}{d^2}\right), P = P_0 + \rho_0 a_0 u \quad (16) \\ \rho &= \rho_0 + \frac{\rho_0}{a_0} u \quad , \quad T = \frac{P}{\rho r} \end{aligned}$$

where $\rho_0 = 0.24$ kg/m^3 and $a_0 = 734.6$ m/s are the mass density and sound speed in the unperturbed initial solution. The sign of the velocity is chosen so that the wave travels in the domain towards positive x values. Periodic boundary conditions are prescribed. Temperature time evolution at $x = 0$ is plotted in Fig. 1. The same temperature field is predicted by both tabulated chemistry and multi-component simulations. Similar conclusions are observed for pressure, velocity and mass density time evolutions.

5.2. Characteristic boundary conditions validation

The NSCBC modifications for tabulated chemistry described in section 4 are tested by injecting acoustic and entropic waves through inflow and outflow boundary conditions. The wave amplitudes $\mathscr{L}_m$ are imposed following the procedure described in Ref. [16].

In the proposed test cases, the initial mixture fraction is given by:

$$z = z_0 + z', \quad \text{with} \quad z_0 = 1 - \frac{x}{L} \qquad (17)$$

where z' is a perturbation. When the flow is not perturbed by acoustic, species and temperature profiles are deduced using Eqs. (14) and (15), respectively. Figure 2 shows species and temperature profiles in this situation and without mixture fraction perturbation ($z' = 0$).

Acoustic wave through subsonic non-reflective outlet (right). An acoustic wave defined by Eq. (16) with parameters: $A = 0.01 a_0$, $d = 2.5\ 10^{-3}$ m and $x_0 = 0.025$ m is superimposed. In this first case, the mixture fraction field is not perturbed: $z' = 0$. Fig. 3 shows velocity and pressure profiles passing through the right boundary. Identical solutions are observed in both multi-component and tabulated chemistry simulations.

Entropic wave through subsonic non-reflective outlet (right). The flow velocity is now uniformly initialized: $u = 20$ m.s^{-1} and $P = 1$ atm. The mixture fraction is perturbed by:

$$z'(x, t=0) = A \exp\left(-\frac{(x-x_0)^2}{d^2}\right) \qquad (18)$$

where $A = -0.5$, $d = 2.5\ 10^{-3}$ m and $x_0 = 0.025$ m. Fig. 4 shows methane mass fraction, temperature and density at different instants. Species mass fractions are transported in the multi-component simulation and extracted from the look-up table in the tabulated chemistry simulation. The entropic wave exits properly the computational domain without introducing numerical artifacts in both multi-component and tabulated chemistry simulations.

5.3. 3-D large eddy simulation of a round jet in a coflow

Validation of the TTC method is addressed here on a three-dimensional simulation of a round jet impinging in a vitiated coflow. The configuration is identical to Ref. [18]. The fuel jet diameter d is 4.57 mm and the bulk velocity V_{jet} is 100 m/s (Reynolds number is 28,000). The coflow velocity is 5.4 m/s. Composition of the fuel jet and the coflow are the same as specified in Tab. 1. Large Eddy Simulation (LES) is performed with multi-component and tabulated chemistry formulations without taking combustion into account. Therefore, only the mixing phenomenon is studied here. The subgrid LES flux is modeled using the WALE model [21]. The domain of length $L = 0.7$ m and of diameter 0.35 m is discretized on a non-uniform mesh composed of 30 million tetrahedra.

An instantaneous mixture fraction isosurface obtained by the tabulated chemistry method is represented in Fig. 5. Instantaneous data are averaged during a physical time equal to one convective time L/V_{jet} to compute mean and root-mean-square (rms) quantities. Figure 6(a) shows that mean axial temperature and rms profiles obtained by both simulations are similar. Same behavior are observed in Fig. 6(b) for radial profiles of mean species mass fraction.

Error in temperature estimation due to the first order truncation of the energy Taylor expansion in Eq. (5) is determined. The bias $B = (T^{TTC} - T^{ref})/T^{ref}$ is introduced. T^{TTC} and T^{ref} are both computed from the transported energy e of the tabulated chemistry simulation. T^{TTC} is estimated from Eq. (5) while T^{ref} is computed using a more expensive iterative algorithm without truncation assumption. In the present 3D LES, the maximum error in the whole computational domain remains very low: Max(B)=0.3%.

5.4. One-dimensional laminar premixed flame with tabulated chemistry

A simulation with combustion is now considered. The TTC method is compatible with any tabulated chemistry model. It is here illustrated with the FPI method [7, 13]. The objective is to simulate a one-dimensional laminar premixed flame with tabulated chemistry method in a compressible CFD code. The reference solution with detailed chemistry is computed with the PREMIX code [22] for a stoichiometric methane-air mixture. In PREMIX, pressure is fixed to 1 atm and fresh gas temperature is 298K. Transport is described with Fick law and unity Lewis numbers for all species. The detailed mechanism GRI 3.0 [23] which involves 53 species is used. The flame structure is tabulated following the FPI methodology [7]. All thermochemical quantities are stored in a look-up table in term of a unique coordinate: $n = 1$ and $\psi_1 = c$ where the progress variable c is defined as the coordinate of the chemical database:

$$c = \frac{Y_{CO_2}}{Y_{CO_{2eq}}} \tag{19}$$

where $Y_{CO_{2eq}}$ is the equilibrium value of CO_2 in burnt gases. AVBP initial solution is obtained by interpolating the detailed chemistry solution profile of c on a mesh with a length $L = 0.04$ m. At the beginning of the computation, an acoustic bump is created and exits the domain because the isobaric CHEMKIN solution is not compatible with a fully compressible formulation.

A convective time is defined as $\tau_{conv} = L/S_l$. The tabulated chemistry simulation runs over a physical time equal to $0.2\ \tau_{conv} = 27$ ms. Comparisons between PREMIX and AVBP solutions are shown in Fig. 7. Species mass fractions and temperature match perfectly, demonstrating the performance of the temperature and boundary condition corrections proposed. Moreover, CPU saving is important since 53 species transport equations are replaced by one balance equation for progress variable.

In this reactive case, the maximum temperature estimation error is Max(B)=0.15%. Figure 7(a) shows the pressure profile accross the flame front. The pressure drop ΔP due to the variation of momentum flux $\Delta(\rho u^2)$ across the deflagration wave is clearly visible.

6. Conclusion

In the present study, we have developed a new technique called TTC (Tabulated Thermochemistry for Compressible flows) to accurately couple tabulated chemistry with compressible flow solvers. A corrective term is proposed to take into account the deviation between the temperature stored in the chemical database and the one calculated in the CFD solver, due to compressible effects. NSCBC boundary conditions are adapted to tabulated chemistry formalism. It is shown that acoustic and entropic waves propagations are very well predicted. A LES of a turbulent round jet shows that the mixing is well described using this new coupling technique with the same accuracy as the multi-component formalism. Finally, a laminar flame simulation shows that the method perfectly reproduces premixed combustion phenomena. This new procedure to efficiently introduce tabulated chemistry in compressible flow solvers enables to take into account detailed chemistry effects in realistic LES configurations.

Acknowledgment

This work was supported by the project ANR-PANH and performed using HPC resources from GENCI-IDRIS (Grant 2009-x2009020164).

References

[1] M. Boileau, G. Staffelbach, B. Cuenot, T. Poinsot, C. Bèrat, Combust. Flame 154 (1-2) (2008) 2–22.
[2] V. Raman, H. Pitsch, Combust. Flame 142 (4) (2005) 329–347.
[3] S. Undapalli, S. Srinivasan, S. Menon, Proc. Combust. Ins. 32 (1) (2009) 1537–1544.
[4] Y. Mizobuchi, S. Tachibana, J. Shinjo, S. Ogawa, T. Takeno, Proceedings of the Combustion Institute 29 (2002) 2009–2015.
[5] E. Hawkes, J. Chen, Combust. Flame 138 (3) (2004) 242–258.
[6] U. Maas, S. B. Pope, Combust. Flame 88 (3-4) (1992) 239–264.
[7] O. Gicquel, N. Darabiha, D. Thevenin, Proceedings of the Combustion Institute 28 (Part 2) (2000) 1901–1908.
[8] J. van Oijen, L. de Goey, Combust. Sci. Technol. 161 (2000) 113–137.
[9] V. Bykov, U. Maas, Comb. Theory Modell. 11 (6) (2007) 839–862.
[10] Z. Ren, S. Pope, A. Vladimirsky, J. Guckenheimer, J. Chem. Phys. 124 (11) (2006).
[11] A. Kempf, H. Forkel, J. Y. Chen, A. Sadiki, J. Janicka, Proceedings of the Combustion Institute 28 (1) (2000) 35–40.
[12] B. Fiorina, R. Baron, O. Gicquel, D. Thevenin, S. Carpentier, N. Darabiha, Comb. Theory Modell. 7 (2003) 449–470.
[13] B. Fiorina, O. Gicquel, L. Vervisch, S. Carpentier, N. Darabiha, Proceedings of the Combustion Institute 30 (2005) 867–874.
[14] J. Galpin, A. Naudin, L. Vervisch, C. Angelberger, O. Colin, P. Domingo, Combust. Flame 155 (1-2) (2008) 247–266.
[15] T. J. Poinsot, S. K. Lele, J. Comput. Phys. 101 (1) (1992) 104–129.
[16] M. Baum, T. Poinsot, D. Thevenin, J. Comput. Phys. 116 (2) (1995) 247–261.
[17] K. Thompson, J. Comput. Phys. 68 (1) (1987) 1–24.
[18] R. Cabra, J. Y. Chen, R. W. Dibble, A. N. Karpetis, R. S. Barlow, Combust. Flame 143 (4) (2005) 491–506.
[19] V. Moureau, G. Lartigue, Y. Sommerer, C. Angelberger, O. Colin, T. Poinsot, J. Comput. Phys. 202 (2) (2005) 710–736.

[20] O. Colin, M. Rudgyard, J. Comput. Phys. 162 (2) (2000) 338–371.
[21] F. Nicoud, F. Ducros, Flow Turbulence Combust. 62 (3) (1999) 183–200.
[22] R. J. Kee, J. F. Grear, M. D. Smooke, J. A. Miller, Tech. Rep. SAND85-8240, Sandia National Laboratories (1985).
[23] http://www.me.berkeley.edu/gri_mech

Fuel side ($z = 1$)		Oxidizer side ($z = 0$)	
T_f	= 320 K	T_{ox}	= 1350 K
Y_{O2_f}	= 0.195	$Y_{O2_{ox}}$	= 0.142
Y_{N2_f}	= 0.591	$Y_{N2_{ox}}$	= 0.758
Y_{H2O_f}	= 0.0	$Y_{H2O_{ox}}$	= 0.1
Y_{CH4_f}	= 0.214	$Y_{CH4_{ox}}$	= 0.0
ϕ_{CH_4}	= 4.4	ϕ_{H_2}	= 0.4

Table 1: Temperature, species mass fractions and equivalence ratio ϕ on fuel and oxidizer sides in the Cabra burner [18].

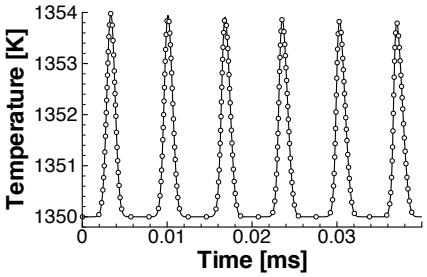

Figure 1: Time variation of temperature at $x = 0$ in the acoustic wave propagation test case. The initial gaussian profile is parametrized by $A = 0.01a_0$, $d = 5\ 10^{-4}$ m and $x_0 = 0.0025$ m. Symbols: multi-component solution. Line: tabulated chemistry solution.

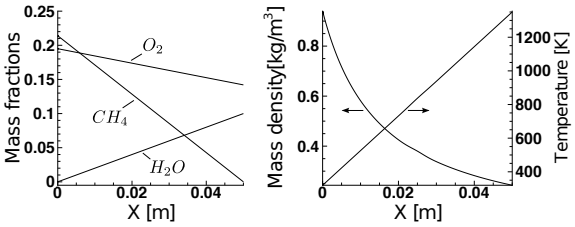

Figure 2: Initial unperturbed solution for NSCBC tests. (a) Species mass fractions. (b) Mass density and temperature.

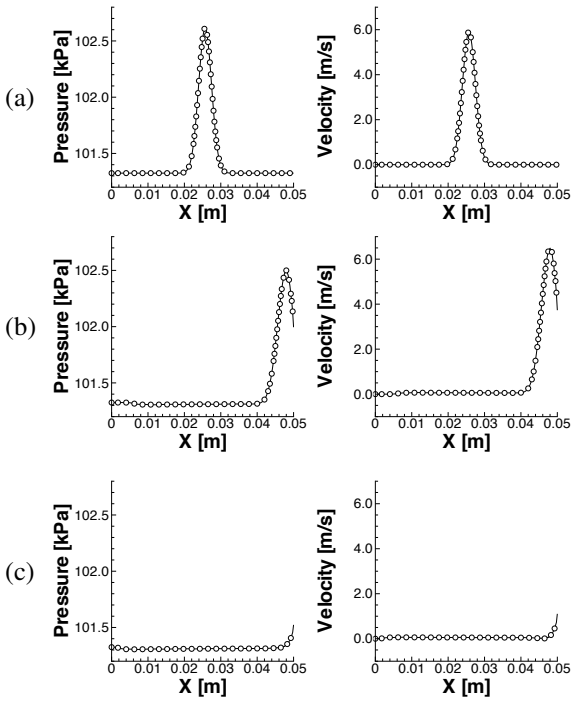

Figure 3: Acoustic wave passing through a non-reflective boundary. Pressure (left) and velocity (right) profiles are plotted for multi-component (symbols) and tabulation (line) formalism at different times $t^+ = tL/a_0(x = L/2)$ in the simulation. (a) Initial solution, $t^+ = 0$; (b) $t^+ = 0.4$; (c) $t^+ = 0.51$.

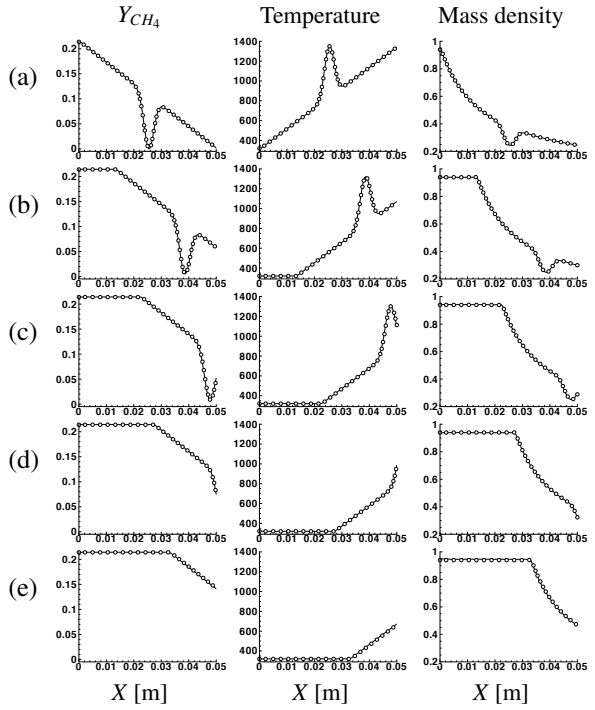

Figure 4: Composition wave passing through a reflective boundary. Methane mass fraction, temparature [K] and mass density [kg/m^3] profiles are plotted for multi-component (symbols) and tabulation (line) formalism at different times $t^+ = tL/u_0$ in the simulation. (a) Initial solution, $t^+ = 0$; (b) $t^+ = 0.27$; (c) $t^+ = 0.45$; (d) $t^+ = 0.54$; (e) $t^+ = 0.63$.

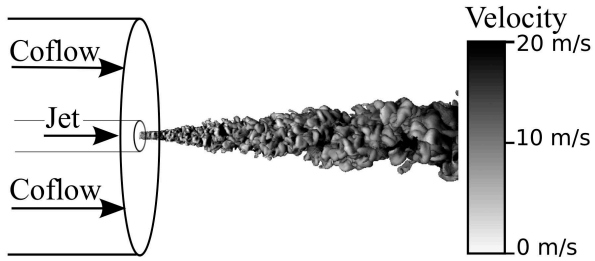

Figure 5: Mixture fraction isosurface $z = 0.1$ colored by longitudinal velocity.

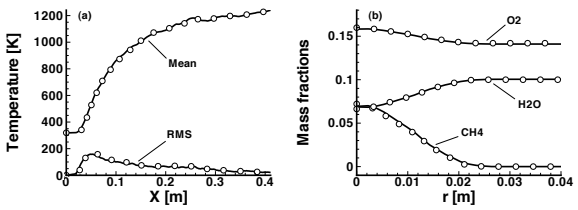

Figure 6: LES Comparison using multi-component (symbols) and tabulated chemistry (line) formulation. (a) Longitudinal mean and root-mean-square (rms) temperature profile. (b) Radial profiles of mean species mass fractions extracted at the axial distance $X = 30d$.

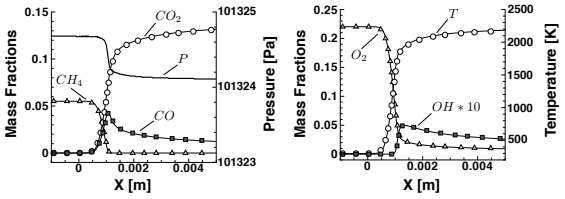

Figure 7: Mass fractions and temperature in a 1-D stoichiometric laminar premixed methane-air flame. Symbols: detailed chemistry solution. Line: tabulated chemistry.

List of Figures